The Canadian Mineralogist
Vol. 47, pp. 1245-1255 (2009)
DOI: 10.3749/canmin.47.5.1245

THE ORTHORHOMBIC STRUCTURE OF $CaCO_3$, $SrCO_3$, $PbCO_3$ AND $BaCO_3$: LINEAR STRUCTURAL TRENDS

SYTLE M. ANTAO§

Department of Geoscience, University of Calgary, Calgary, Alberta T2N 1N4, Canada

ISHMAEL HASSAN

Department of Chemistry, University of the West Indies, Mona, Kingston 7, Jamaica

ABSTRACT

The crystal structures of four isostructural orthorhombic carbonates, $CaCO_3$ (aragonite), $SrCO_3$ (strontianite), $PbCO_3$ (cerussite), and $BaCO_3$ (witherite), were obtained by Rietveld refinements using data acquired by synchrotron high-resolution powder X-ray diffraction (HRPXRD). For $BaCO_3$, powder neutron-diffraction data were obtained and refined by the Rietveld method. For aragonite, we also carried out a refinement of the structure by single-crystal X-ray diffraction. These carbonates belong to the space group *Pmcn*, with Z = 4. The CO_3 group is slightly non-planar, and the two independent C–O distances are slightly different. The CO_3 group becomes more symmetrical and less aplanar from $CaCO_3$ to $BaCO_3$ (M^{2+}_{radii}: Ca < Sr < Pb < Ba). The $CaCO_3$ structure is, therefore, the most distorted, whereas the $BaCO_3$ structure is the least distorted. Several linear structural trends are observed in plots of selected parameters as a function of the unit-cell volume, *V*. These parameters are radii of the nine-coordinated M^{2+} cations, the unit-cell axes, the average <*M*–O> and <C–O> distances, average <O–C–O> angle, and aplanarity. These linear trends are the result of the effective size of the divalent ionic radius of the *M* cations that are coordinated to nine oxygen atoms. The geometrical features of the CO_3 group can be obtained reliably only by using neutron-diffraction data, especially in the presence of other heavy atoms.

Keywords: $CaCO_3$, aragonite, $SrCO_3$, strontianite, $PbCO_3$, cerussite, $BaCO_3$, witherite, Rietveld refinements, synchrotron high-resolution powder X-ray diffraction (HRPXRD), neutron diffraction, crystal structure.

SOMMAIRE

Nous avons affiné la structure cristalline de quatre carbonates orthorhombiques isostructuraux, $CaCO_3$ (aragonite), $SrCO_3$ (strontianite), $PbCO_3$ (cérusite), et $BaCO_3$ (witherite), par la méthode de Rietveld en utilisant les données acquises par diffraction X à haute résolution avec rayonnement synchrotron. Pour le $BaCO_3$, nous avons utilisé des données obtenues par diffraction neutronique, aussi affinées par la méthode de Rietveld. Pour l'aragonite, nous avons affiné la structure par diffraction X sur monocristal. Ces carbonates répondent au groupe spatial *Pmcn*, avec Z = 4. Le groupe CO_3 est légèrement non planaire, et les deux distances C–O indépendantes diffèrent légèrement. Le groupe CO_3 devient plus symétrique et moins aplanaire en allant de $CaCO_3$ à $BaCO_3$ (M^{2+}_{rayon}: Ca < Sr < Pb < Ba). La structure de $CaCO_3$ serait donc la plus difforme, tandis que la structure de $BaCO_3$ serait la moins difforme. Plusieurs tendances structurales sont évidentes dans les tracés de paramètres choisis en fonction du volume de la maille élémentaire, *V*. Parmi ces paramètres sont le rayon des cations M^{2+} à coordinence neuf, les dimensions le long des axes de la maille élémentaire, les distances <*M*–O> et <C–O> moyennes, l'angle <O–C–O> moyen, et l'aplanarité. Ces tracés linéaires sont le résultat de la dimension effective du rayon ionique du cation *M* bivalent coordonné aux neuf atomes d'oxygène. On ne peut évaluer les aspects géométriques du groupe CO_3 qu'avec les données en diffraction neutronique, surtout en présence des atomes lourds dans la structure.

(Traduit par la Rédaction)

Mots-clés: $CaCO_3$, aragonite, $SrCO_3$, strontianite, $PbCO_3$, cérusite, $BaCO_3$, withérite, affinements de Rietveld, diffraction X à haute résolution avec rayonnement synchrotron, diffraction neutronique, structure cristalline.

§ *E-mail address*: antao@ucalgary.ca

Introduction

The naturally occurring isostructural orthorhombic carbonates are aragonite ($CaCO_3$), strontianite ($SrCO_3$), cerussite ($PbCO_3$), and witherite ($BaCO_3$), listed with increasing size of the M^{2+} cation. In addition, isostructural rare-earth and radium carbonates ($YbCO_3$, $EuCO_3$, $SmCO_3$, and $RaCO_3$) have been synthesized (Speer 1983). Linear structural trends are expected to occur in these series; their crystal structures were examined previously, but only general trends were observed (De Villiers 1971, Chevrier *et al.* 1992). The M^{2+} cations should have some effect on the slightly aplanar CO_3 group and on the two independent but slightly different C–O distances, although CO_3 groups are generally considered to be rigid. With X-ray diffraction, it is difficult to accurately locate light atoms such as C in the presence of heavy atoms such as Pb (including problems from absorption). For this reason, neutron-diffraction experiments were performed on aragonite, strontianite, and cerussite (Chevrier *et al.* 1992, Jarosch & Heger 1986, 1988), but not on witherite. The apparent lack of linear trends to date seems to arise from an inappropriate choice of a structural parameter against which to plot suitable structural variables.

Although the structure of aragonite is well established and has been accepted for a long time, the findings of Bevan *et al.* (2002) on a sample that contains a small amount of Sr atom was unexpected. They refined the structure of a twinned crystal of aragonite from an unknown locality in space group $P\bar{1}$, and cast some doubt about the structures of aragonite that were refined in space group *Pmcn*. The present structure of aragonite was refined in order to resolve some of this controversy. Refinement data for two aragonite samples from localities different than those sampled by other investigators were also obtained.

The purpose of this study is to examine the structural trends in the orthorhombic carbonates $CaCO_3$, $SrCO_3$, $PbCO_3$, and $BaCO_3$ using Rietveld structure refinements and synchrotron high-resolution powder X-ray-diffraction (HRPXRD) data. We also studied by neutron diffraction the structure of $BaCO_3$. In addition, we refined the structure of one aragonite sample using a single-crystal approach. The results from the present study gave linear structural trends across the series.

Background Information

Aragonite, the most common orthorhombic carbonate, occurs as the inorganic constituent of many invertebrate skeletons and sediments derived from them. It also occurs as a primary phase in high-pressure metamorphic rocks. The crystal structure of aragonite was determined by Bragg (1924) and Wyckoff (1925). Subsequently, several refinements were carried out (Dal Negro & Ungaretti 1971, De Villiers 1971, Dickens & Bowen 1971, Jarosch & Heger 1986, Bevan *et al.* 2002, Caspi *et al.* 2005, Pokroy *et al.* 2007). Pilati *et al.* (1998) carried out lattice-dynamic studies on several carbonates. The structures of aragonite were refined in space group *Pmcn*, except for one structure refined in the triclinic system, space group $P\bar{1}$, by Bevan *et al.* (2002).

The crystal structure of strontianite was determined by Zachariasen (1928), and refined by De Villiers (1971) and Jarosch & Heger (1988), whereas the crystal structure of witherite was determined by Colby & La Coste (1933) and refined by others (De Villiers 1971, Holl *et al.* 2000).

Studies of the isostructural orthorhombic carbonate phases are important in understanding the transition sequences in $CaCO_3$ and may provide insights into the behavior of carbon in the mantle (*e.g.,* Berg 1986, Antao *et al.* 2004). Because of the importance of CO_2 sequestration and possible order–disorder of cations and CO_3 groups, we have recently examined the crystal structures of several carbonates (Antao *et al.* 2004, 2008a, 2009, Antao & Hassan 2007). In addition, results of several high-pressure studies are available for $CaCO_3$, $BaCO_3$ and $SrCO_3$ (Lin & Liu 1997, Holl *et al.* 2000, Santillán & Williams 2004, Ono 2007).

Experimental Methods

Sample characterization

One sample of aragonite used in this study is from Tuscany, Italy, and occurs as colorless needle-like crystals that occur in a cavity. The chemical analysis of this aragonite (using small crystals encapsulated in epoxy resin, polished, and carbon coated) was done using a Cameca Camebax electron microprobe (EMP) using the operating program MBX (copyright by Carl Henderson, University of Michigan); the correction was done using Cameca's PAP program. The analytical conditions were 15 kV, and with a beam current of 9.6 nA. A diffuse beam of electrons was used for the analysis to avoid volatilization. Minerals were used as standards [*e.g.,* dolomite (Ca$K\alpha$, Mg$K\alpha$), siderite (Fe$K\alpha$), and rhodonite (Mn$K\alpha$)]. Typical oxide weight percentages resulting from the EMP analyses are given (Table 1). The chemical formula obtained for this aragonite is $Ca_{0.996}Mg_{0.001}Sr_{0.003}CO_3$, which is close to the ideal formula, $CaCO_3$. The average amount of Sr, in atoms per formula unit (*apfu*), is 0.005, with minimum and maximum values ranging from 0 to 0.007 *apfu*.

The other aragonite sample is from Cuenca, Spain; it occurs as a large (several cm in size) euhedral crystal hexagonal in shape. This aragonite sample was analyzed in a similar manner (Table 1), and the formula is $Ca_{0.985}Sr_{0.014}CO_3$. The average amount of Sr is 0.014 atoms per formula unit (*apfu*), with minimum and maximum values ranging from 0.012 to 0.015 *apfu*. This amount of Sr is about three times more than that in the sample from Italy.

The other materials ($PbCO_3$, $BaCO_3$ and $SrCO_3$) were obtained as high-purity (99.999%) reagent-grade powders and were assumed to be pure. The formula MCO_3 was used in the structure refinements below.

Single-crystal X-ray-diffraction study of aragonite from Tuscany, Italy

A single-crystal fragment from the Italian sample was selected under a binocular microscope for structure refinement using a Bruker P4 automated four-circle single-crystal X-ray diffractometer with a SMART–CCD detector and graphite-monochromatized Mo$K\alpha$ radiation generated at 50 kV and 30 mA. We recorded our data with an exposure time of 30 s per frame, with a detector distance of 5.016 cm. Five sections of frames were collected with a step width of 0.30° in φ. All data were integrated using SAINT (Bruker 2000), and empirical absorption corrections were performed using SADABS (Sheldrick 2001). The data were also corrected for Lorentz, polarization, and background effects. The unit-cell parameters were calculated and refined from all the intensities with $I > 15\sigma(I)$. However, the cell parameters used in the single-crystal structure refinement were those obtained from Rietveld refinement using synchrotron HRPXRD data because this approach provides more accurate cell parameters (see below). The structure refinement was done using the SHELXTL97 suite of programs (Sheldrick 1997). The refinements were carried out by varying the parameters in the following sequence: scale, atom positions, isotropic, and anisotropic displacement parameters. The cell parameters and other information regarding data collection, criteria for observed reflections, and refinement are given in Tables 2a and 2b. The space group *Pmcn* was used in this study, and no reflections were observed that violate this space group. Finally, all variables were refined simultaneously to an R factor of 0.0277. The atom positions and isotropic displacement parameters are given in Table 3a. Anisotropic displacement parameters are given in Table 3b. Selected bond distances and angles are given in Table 4. Table 5 contains observed and calculated structure-factors; it is available from the Depository of Unpublished Data on the MAC website [document Aragonite CM47_1245].

TABLE 1. ARAGONITE: RESULTS OF ELECTRON-MICROPROBE ANALYSES

	Tuscany, Italy	Cuenca, Spain		Tuscany, Italy	Cuenca, Spain
CaO wt%	55.27	54.98	Ca *apfu*	0.996	0.985
FeO	0.01	0.01	Fe	0.000	0.000
MnO	0.03	0.00	Mn	0.000	0.000
MgO	0.02	0.00	Mg	0.001	0.000
SrO	0.31	1.49	Sr	0.003	0.014
BaO	0.00	0.02	Ba	0.000	0.000
ZnO	0.00	0.00	Zn	0.000	0.000
† CO_2	43.56	43.79	†(CO_3)	1.0	1.0
Total	99.20	100.30			

† Calculated from stoichiometry. HRPXRD data were obtained for both aragonite samples, single-crystal (SXTL) data were obtained only for the Tuscany sample.

Synchrotron high-resolution powder X-ray diffraction (*HRPXRD*)

Five samples (synthetic $SrCO_3$, $PbCO_3$, $BaCO_3$ and the two natural aragonite samples) were studied by HRPXRD. The experiments were performed at beamline 11–BM, Advanced Photon Source (APS), Argonne National Laboratory (ANL). Each sample was crushed (for about 5 minutes) to a fine powder using an agate mortar and pestle. The samples were loaded into kapton capillaries and rotated during the experiment at a rate of 90 rotations per second. The data were collected

TABLE 2a. CELL PARAMETERS AND RIETVELD REFINEMENT STATISTICS FOR ORTHORHOMBIC CARBONATES

	$CaCO_3$ Italy SXTL§	$CaCO_3$ Italy HRPXRD	$CaCO_3$ Spain HRPXRD	$SrCO_3$ synthetic HRPXRD	$PbCO_3$ synthetic HRPXRD	$BaCO_3$ synthetic HRPXRD	$BaCO_3$ synthetic Neutron
a (Å)	4.96062(2)	4.96062(2)	4.96174(2)	5.107499(2)	5.18324(2)	5.31459(1)	5.31640(8)
b (Å)	7.97006(7)	7.97006(7)	7.96918(3)	8.413820(3)	8.49920(3)	8.90428(2)	8.9056(1)
c (Å)	5.74181(3)	5.74181(3)	5.74265(2)	6.026924(2)	6.14746(3)	6.43409(2)	6.43383(7)
V (Å^3)	227.011(2)	227.011(2)	227.070(1)	258.9985(2)	270.817(2)	304.478(1)	304.614(8)
λ (Å)	0.71073	0.401649(2)	0.40245(2)	0.40172(2)	0.40231(2)	0.40167(2)	
*R_F^2	0.0277	0.0399	0.0369	0.0318	0.0579	0.0316	0.0882
N_{obs}	793	700	699	750	656	922	1381
2θ range	8-90°	0-40°	0-40°	0-40°	0-40°	0-40°	

*R_F^2 : R-structure factor based on observed and calculated structure-amplitudes = $[\Sigma(F_o^2 - F_c^2) / \Sigma(F_o^2)]^{1/2}$; § SXTL: single-crystal data, cell parameters from HRPXRD, and R1 is given. Space group is *Pmcn*, and the number of formula units per unit cell Z is 4. The Caspi *et al.* (2005) cell parameters for a crystal of aragonite from Sefrou, Morocco are: *a* 4.96183(1), *b* 7.96914(2), *c* 5.74285(2) Å, *V* 227.081(1) Å^3, which is remarkably similar to that from Spain (within 2 × 10^{-4} Å).

to a maximum 2θ of about 40° with a step size of 0.0005° and a step time of 0.2 s per step. The HRPXRD traces were collected with twelve silicon (111) crystal analyzers that increase detector efficiency, reduce the angular range to be scanned, and allow rapid acquisition of data. A silicon and alumina NIST standard (ratio of $^1/_3$ Si : $^2/_3$ Al_2O_3) was used to calibrate the instrument and to determine and refine the wavelength used in the experiment. Additional details of the experimental set-up are given elsewhere (Antao *et al*. 2008b, Lee *et al*. 2008, Wang *et al*. 2008).

Neutron powder-diffraction refinement of $BaCO_3$

Time-of-flight neutron-diffraction measurements on $BaCO_3$ were performed using the Special Environment Powder Diffractometer (SEPD) of the Intense Pulsed Neutron Source (IPNS) at ANL. About 8 g of sample was packed into a vanadium can; data were collected at ambient conditions over a period of three hours.

Rietveld structure refinements

To extract structural parameters, the measured HRPXRD and neutron profiles were analyzed by the Rietveld method (Rietveld 1969), as implemented in the GSAS program (Larson & Von Dreele 2000), and using the EXPGUI interface (Toby 2001). Scattering curves for neutral atoms were used in all refinements. The starting coordinates of all atoms, the cell parameters, and the space group, *Pmcn*, were taken from De Villiers (1971). The background was modeled using a Chebyschev polynomial. The reflection-peak profiles were fitted using type-3 profile in the GSAS program. Full-matrix least-squares refinements were carried out by varying the parameters in the following sequence: a scale factor, cell parameters, atom coordinates, and isotropic displacement parameters. Toward the end of the refinement, all the parameters were allowed to vary simultaneously, and the refinement proceeded to convergence. The HRPXRD traces are shown in Figures 1 and 2. No reflections violating space group *Pmcn* were observed in this study, which is in contrast to the work on a different sample of aragonite (Bevan *et al*. 2002). The neutron diffraction pattern for $BaCO_3$ is shown in Figure 3.

The cell parameters and the Rietveld refinement statistics are listed in Table 2a. Atom positions and isotropic displacement parameters are given in Table 3a. Bond distances and angles are given in Table 4.

TABLE 2b. DATA ON SINGLE-CRYSTAL (SXTL) STRUCTURE REFINEMENT OF ARAGONITE FROM TUSCANY, ITALY

Empirical formula	$CaCO_3$	Absorption coeff.	2.465 mm^{-1}
Z	4	F(000)	200
Formula weight	400.36	Crystal size	0.2 × 0.1 × 0.05 mm^3
Temperature	293(2) K	Theta range for data collection	4.37 to 46.38°
Density (calculated)	2.929 Mg/m^3		
Index ranges		$-9 \le h \le 9$, $-14 \le k \le 14$, $-9 \le l \le 9$	
Reflections collected		3454	
Independent reflections		793 [R(int) = 0.0450]	
Absorption correction		Empirical, using SADABS	
Refinement method		Full-matrix least-squares on F^2	
Data / restraints / parameters		793 / 0 / 29	
Goodness-of-fit on F^2		0.987	
Final R indices [I>2σ(I)]		R1 = 0.0277, wR2 = 0.0643	
R indices (all data)		R1 = 0.0328, wR2 = 0.0659	
Extinction coefficient		0.041(9)	
Largest diff. peak and hole		0.595 and -0.806 $e.Å^{-3}$	

TABLE 3a. POSITIONS* AND ISOTROPIC DISPLACEMENT PARAMETERS ($Å^2$) OF ATOMS IN ORTHORHOMBIC CARBONATES

Atom		$CaCO_3$ Italy SXTL	$CaCO_3$ Italy HRPXRD	$CaCO_3$ Spain HRPXRD	$SrCO_3$ synthetic HRPXRD	$PbCO_3$ synthetic HRPXRD	$BaCO_3$ synthetic HRPXRD	$BaCO_3$ synthetic Neutron
M	*y*	0.4150(1)	0.41502(5)	0.41508(3)	0.41623(1)	0.41739(3)	0.41639(2)	0.4166(2)
	z	0.7596(1)	0.7577(1)	0.75953(5)	0.75680(2)	0.7538(1)	0.75436(5)	0.7530(3)
	U	0.008(1)	0.0066(2)	0.00735(6)	0.00630(2)	0.01696(8)	0.00906(4)	0.0044(4)
C	*y*	0.7619(1)	0.7616(3)	0.7612(1)	0.7584(1)	0.7541(10)	0.7556(3)	0.7555(2)
	z	-0.0849(2)	-0.0808(3)	-0.0842(2)	-0.0861(2)	-0.080(1)	-0.0783(4)	-0.0817(3)
	U	0.008(1)	0.0115(2)	0.0107(1)	0.00931(8)	0.01696(8)	0.00906(4)	0.0083(3)
O1	*y*	0.9224(1)	0.9220(2)	0.9228(1)	0.91133(9)	0.9057(7)	0.9011(2)	0.8999(2)
	z	-0.0956(1)	-0.0944(2)	-0.0947(1)	-0.0943(1)	-0.0907(9)	-0.0894(3)	-0.0923(4)
	U	0.013(1)	0.0115(2)	0.0107(1)	0.00931(8)	0.01696(8)	0.00906(4)	0.0114(4)
O2	*x*	0.4738(1)	0.4750(2)	0.4743(1)	0.46786(9)	0.4638(7)	0.4601(2)	0.4596(2)
	y	0.6804(1)	0.6824(1)	0.68059(6)	0.68167(6)	0.6786(4)	0.6832(1)	0.6831(2)
	z	-0.0871(1)	-0.0905(2)	-0.0871(1)	-0.08653(8)	-0.0824(6)	-0.0820(2)	-0.0794(3)
	U	0.012(1)	0.0115(2)	0.0107(1)	0.00931(8)	0.01696(8)	0.00906(4)	0.0109(3)

* Atomic positions: *M*, C, and O1 at 4*c* (¼, *y*, *z*), and O2 at 8*d* (*x*, *y*, *z*). *M* cations: Ca, Sr, Pb, Ba.

Results and Discussion

Structure of orthorhombic $CaCO_3$, $SrCO_3$, $PbCO_3$, and $BaCO_3$

The phases $CaCO_3$, $SrCO_3$, $PbCO_3$, and $BaCO_3$ are isostructural, and have the aragonite-type structure (Fig. 4). Layers of nine-coordinated M^{2+} (*M*: Ca, Sr, Pb, or Ba) cations are parallel to (001), and the atoms occur approximately in the positions of hexagonal close-packing. This is in contrast with the deformed cubic close-packed arrangement of Ca^{2+} cations in calcite, and gives rise to the pseudo-hexagonal symmetry in these orthorhombic compounds. Successive CO_3^{2-} groups along **c** point alternately to the +**b** and –**b** directions (Fig. 4). Although the M^{2+} cations are nearly in a hexagonal array, the arrangement of the CO_3^{2-} groups lowers the symmetry to orthorhombic, and the CO_3^{2-} groups are slightly aplanar (Table 4).

Linear structural trends

The unit-cell parameters for the isostructural carbonates are in excellent agreement with those obtained previously (*e.g.,* De Villiers 1971, Jarosch & Heger 1986, 1988, Lucas *et al*. 1999, Holl *et al*. 2000). However, cell parameters obtained in this study are significantly more accurate, as they were obtained from HRPXRD data (Table 2a). In general, the high quality of the HRPXRD trace (including both statistics and angular resolution) allows the unit-cell parameters to be determined accurately and reliably.

Using a HRPXRD technique similar to that used in the present study, the structure of an aragonite sample from Sefrou, Morocco was obtained by Caspi *et al*. (2005). Their cell parameters (see footnote to Table 2) are in excellent agreement (within 2×10^{-4} Å) with those for our sample from Spain, and deviate slightly from those for the sample from Italy (within 1×10^{-3} Å). These small differences in cell parameters among aragonite samples arise from different contents of trace elements, in particular Sr; the larger cell volume is associated with larger amounts of Sr. The amount of Sr (*apfu*) in the sample from Spain is about three times more than that from Italy (Table 1). Other studies have also shown that Sr is important in aragonite (Caspi *et al*. 2005, Finch & Allison 2007).

Strontium and Mg atoms in calcite and aragonite are used as proxies of temperature in paleoenvironmental reconstructions. Finch & Allison (2007) used X-ray absorption fine structure (XAFS) to show that Sr substitutes for Ca in aragonite and causes a small (2%) dilation, whereas Sr substitution for Ca in calcite causes a 6.5% dilation.

Although Bevan *et al*. (2002) used $P\bar{1}$ and merohedral twinning to produce a structural model for aragonite, their results cannot be generalized to all samples of aragonite. In particular, their sample of unknown origin contains a small amount of Sr (about 1 atom %), whereas our samples contain minor impurities, as is the case for most samples of aragonite, and give rise to the ideal formula $CaCO_3$ (see Deer *et al*. 1992). Caspi *et al*.

TABLE 3b. ANISOTROPIC DISPLACEMENT PARAMETERS (Å²) FOR ARAGONITE

	U_{11}	U_{22}	U_{33}	U_{23}	U_{13}	U_{12}
Ca	0.009(1)	0.007(1)	0.009(1)	0(1)	0	0
O1	0.016(1)	0.007(1)	0.014(1)	0(1)	0	0
O2	0.009(1)	0.012(1)	0.014(1)	0.001(1)	0.000(1)	0.003(1)
C	0.009(1)	0.009(1)	0.005(1)	0.000(1)	0	0

The anisotropic displacement factor exponent takes the form: $-2\pi^2[h^2a^{*2}U_{11} + ... + 2hka^*b^*U_{12}]$.

TABLE 4. SELECTED INTERATOMIC DISTANCES (Å) AND ANGLES (°) FOR ORTHORHOMBIC CARBONATES

		$CaCO_3$ Italy SXTL	$CaCO_3$ Italy HRPXRD	$CaCO_3$ Spain HRPXRD	$SrCO_3$ synthetic HRPXRD	$PbCO_3$ synthetic HRPXRD	$BaCO_3$ synthetic HRPXRD	$BaCO_3$ synthetic Neutron
M–O1	× 1	2.4164(8)	2.403(1)	2.4097(7)	2.5658(7)	2.597(5)	2.745(2)	2.757(3)
M–O1	× 2	2.6536(3)	2.6521(5)	2.6560(3)	2.7354(3)	2.781(2)	2.865(1)	2.856(1)
M–O2	× 2	2.5459(5)	2.558(1)	2.5478(6)	2.6679(5)	2.678(4)	2.828(1)	2.835(3)
M–O2	× 2	2.4478(5)	2.473(1)	2.4478(6)	2.5893(5)	2.635(4)	2.757(1)	2.754(2)
M–O2	× 2	2.5209(5)	2.494(1)	2.5186(6)	2.6504(5)	2.726(4)	2.813(1)	2.821(2)
<*M*–O> [9]		2.5281(2)	2.5286(3)	2.5278(2)	2.6502(2)	2.693(1)	2.8079(4)	2.8099(7)
C–O1	× 1	1.2810(11)	1.281(2)	1.289(1)	1.288(1)	1.290(9)	1.298(3)	1.288(2)
C–O2	× 2	1.2861(7)	1.284(1)	1.2851(6)	1.2864(6)	1.281(5)	1.290(2)	1.287(1)
<C–O> [3]		1.2844(5)	1.2830(8)	1.2864(4)	1.2869(4)	1.284(4)	1.293(1)	1.2873(8)
O1–C–O2	× 2	120.25(4)	119.2(1)	119.92(5)	120.09(5)	120.0(4)	119.9(1)	120.04(8)
O2–C–O2	× 1	119.34(9)	120.8(2)	120.0(1)	119.8(1)	119.9(8)	120.0(3)	119.9(2)
<O–C–O> [3]		119.95(4)	119.73(8)	119.95(4)	119.99(4)	120.0(3)	119.9(1)	119.99(8)
Aplanarity (Å)		0.030	0.064	0.031	0.018	0.032	0.040	0.013

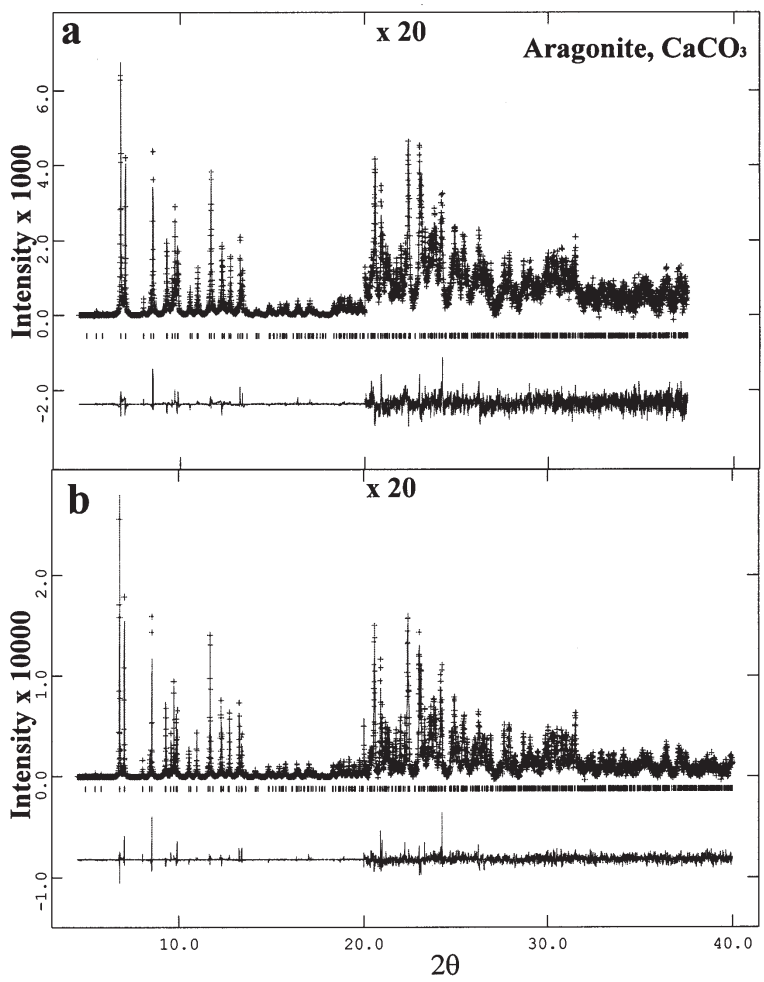

FIG. 1. Comparison of the HRPXRD traces for aragonite, $CaCO_3$, from (a) Tuscany, Italy, and (b) Cuenca, Spain, together with the calculated (continuous line) and observed (crosses) profiles. The difference curve ($I_{obs} - I_{calc}$) is shown at the bottom. The short vertical lines indicate the positions of allowed reflections. In both cases, the intensities beyond 20° 2θ are scaled by a factor of ×20. The FWHM in (a) is more than that in (b).

(2005) did not observe any reflections violating *Pmcn* symmetry, as in our results for both single-crystal and powder samples. In powder X-ray diffraction, twinning effects can be eliminated. The lack of any split or unindexed reflection peaks in our data indicates that a symmetry lower than *Pmcn* is unlikely for end-member aragonite. This is also supported by the single-crystal data for our aragonite sample from Italy.

The radii of the nine-coordinated M^{2+} cations (Shannon 1976) and the *a*, *b*, *c* unit-cell parameters are plotted against the volume, *V* (Fig. 5). Data from the literature are also included in the graphs (see caption to

FIG. 2. Comparison of the HRPXRD traces for $SrCO_3$, $PbCO_3$, and $BaCO_3$, together with the calculated (continuous line) and observed (crosses) profiles. The difference curve ($I_{obs} - I_{calc}$) is shown at the bottom. The short vertical lines indicate the positions of allowed reflections. Note the change in intensity scale at high 2θ, and the factors are given as ×15, *etc*. The FWHM of $SrCO_3$ is the lowest, whereas that of $PbCO_3$ is the highest.

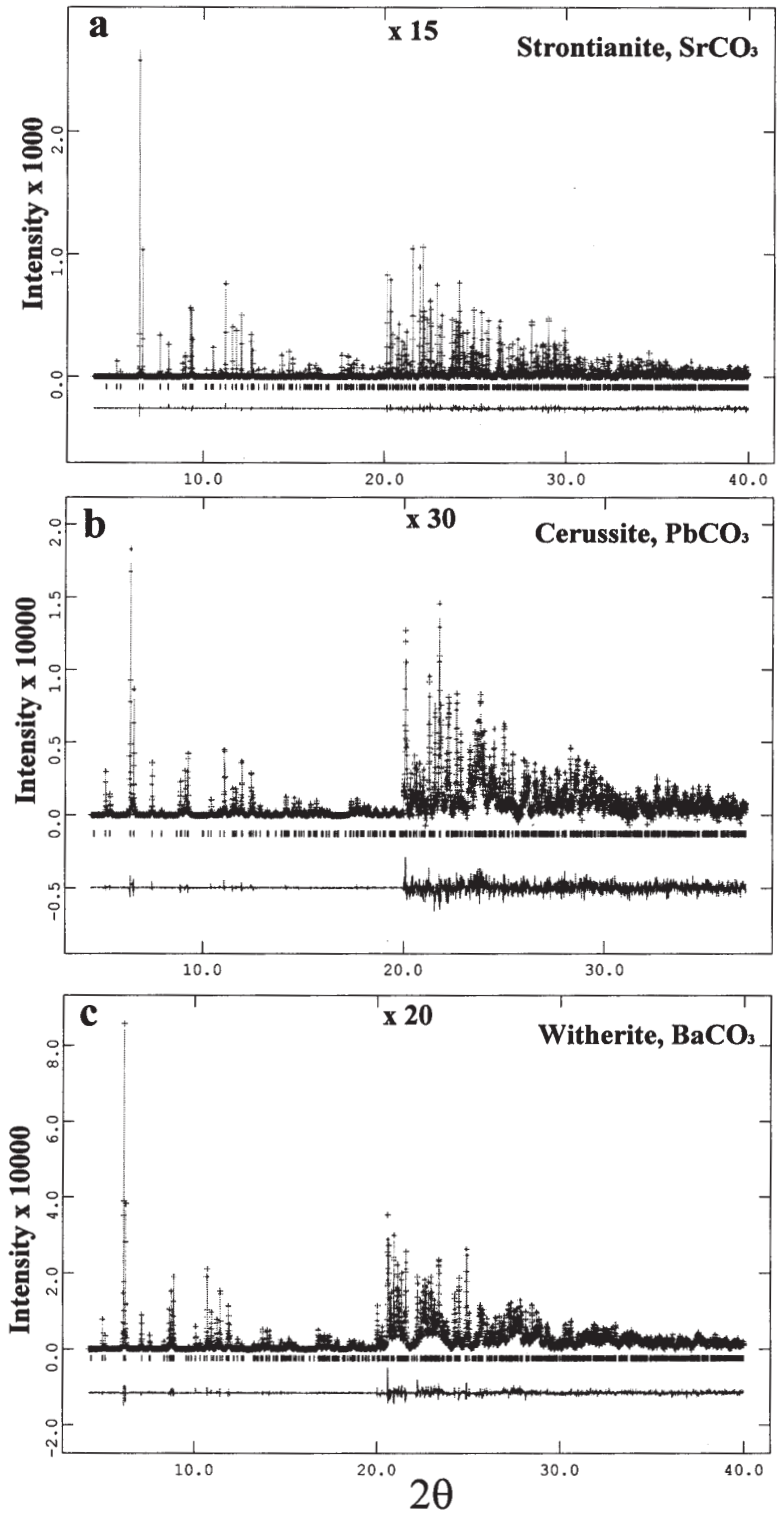
a
x 15
Strontianite, SrCO3
Intensity x 1000
2.0
1.0
0.0
10.0
20.0
30.0
40.0
b
x 30
Cerussite, PbCO3
Intensity x 10000
2.0
1.5
1.0
0.5
0.0
−0.5
10.0
20.0
30.0
c
x 20
Witherite, BaCO3
Intensity x 10000
8.0
6.0
4.0
2.0
0.0
−2.0
10.0
20.0
30.0
40.0
2θ

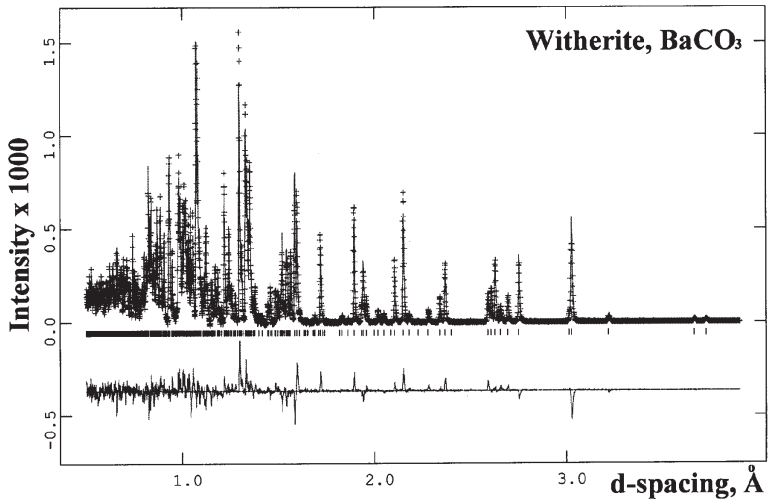

FIG. 3. The neutron diffraction trace for $BaCO_3$, together with the calculated (continuous line) and observed (crosses) profiles. The difference curve ($I_{obs} - I_{calc}$) is shown at the bottom. The short vertical lines indicate the positions of allowed reflections.

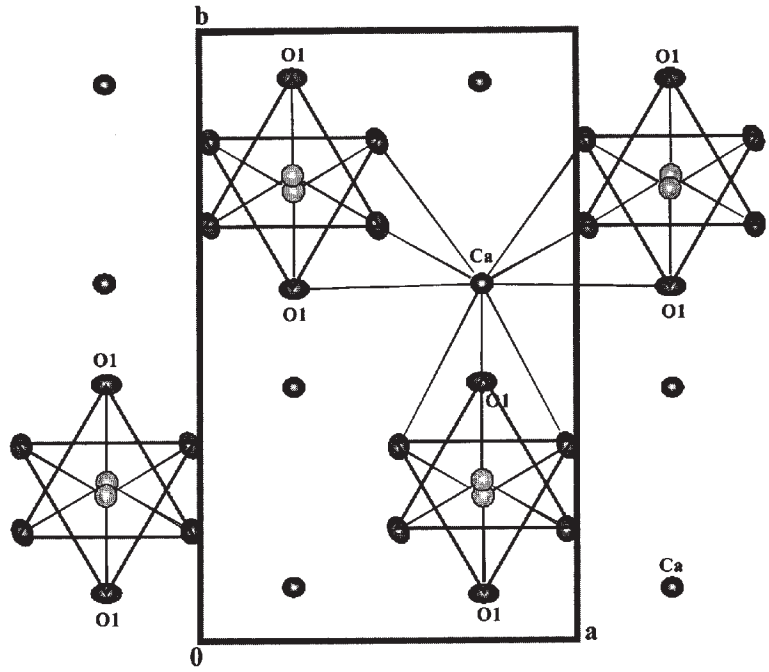

FIG. 4. Projection of the orthorhombic $CaCO_3$ structure showing the approximate hexagonal close-packing of the O atoms and the coordination of a Ca atom to nine O atoms of six different CO_3 groups. The O2 atoms are unlabeled.

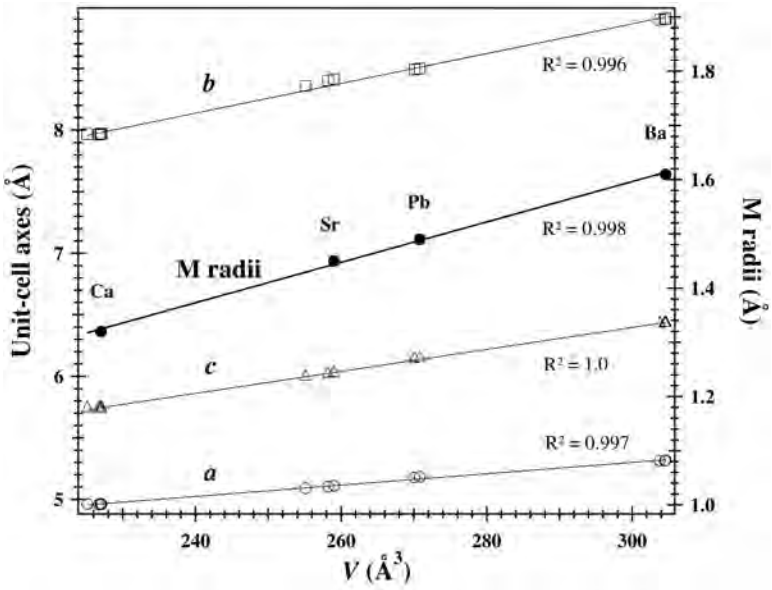

FIG. 5. The radii of the nine-coordinated M^{2+} cations and the *a*, *b*, *c* unit-cell parameters *versus* volume, *V*. They increase linearly. Data are taken from this study and from the literature (Caspi *et al*. 2005, Chevrier *et al*. 1992, Dal Negro & Ungaretti 1971, De Villiers 1971, Jarosch & Heger 1986, 1988, Pokroy *et al*. 2007).

Fig. 5). Linear trends are observed with a R^2 value of 1, its ideal value for an excellent fit (inserts in Fig. 5).

The average <*M*–O> distances are also plotted against *V* (Fig. 6). With all the data included, a linear trend is observed. The present data also show that the *M*–O polyhedra become less distorted with increase in the size of M^{2+} cations, as indicated by De Villiers (1971). That is, the individual *M*–O distances are closer to the mean <*M*–O> distance in $BaCO_3$ than in $CaCO_3$ (Table 4).

The excellent linear fits of the above structural parameters show that reliable cell and <*M*–O> distances can easily be obtained with either X-ray diffraction or neutron diffraction, using either single-crystal or powder samples (Figs. 5, 6). This is not the case for the geometry of the CO_3 group because of the light C atom in the presence of heavy atoms in the aragonite-type structure.

The geometrical features of the CO_3 group are plotted against *V* (Figs. 7a, b, c). Only the data from neutron refinements are shown. If other data were plotted (not shown), there would be considerable scatter, indicating that the C atom position is not located accurately with X-ray diffraction. The structural parameters of the CO_3 group in $PbCO_3$ are shown (as x symbols in graphs), but they do not fall on the trend lines. Those points were not included in the computation of the linear trend lines. It should be noted that the <Pb–O> distance does fall on the expected trend line (Fig. 6), so it appears that the C position may not have been accurately determined in $PbCO_3$.

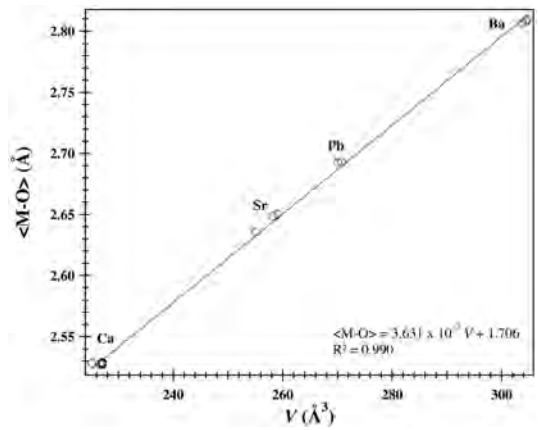

FIG. 6. Linear increase in average <*M*–O> distance with volume, *V*. Data are taken from this study and the literature (see caption to Fig. 5). The equation of the straight line and the goodness-of-fit (R^2) are given as inserts in Figures 6 and 7.

The average <C–O> distance and <O–C–O> angle increase linearly with *V*, whereas the aplanarity of the CO_3 group decreases (Fig. 7). The aplanarity of the CO_3 group is defined by the distance of the C atom from the plane formed by the three O atoms. This CO_3 group thus becomes more symmetrical (C–O distances nearly equal) and less aplanar in going from aragonite to witherite. Therefore, in this isostructural series of materials, the aragonite structure is the most distorted, whereas the witherite structure is the least distorted in terms of the geometry of the CO_3 group and the [MO_9] polyhedron. The structural parameters of this series of phases are influenced and correlated with size of the *M* cations.

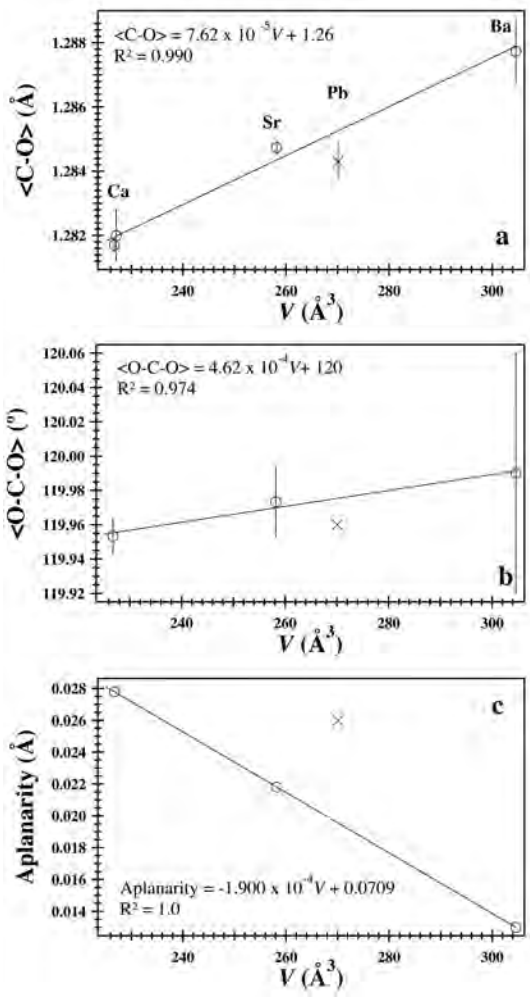

FIG. 7. Neutron-diffraction data for $BaCO_3$ (this study), aragonite (Jarosch & Heger 1986, Pokroy *et al*. 2007), strontianite (Jarosch & Heger 1988), and cerussite (Chevrier *et al*. 1992): (a) <C–O> *versus V*, (b) <O–C–O> *versus V*, and (c) aplanarity *versus V*. Data for $PbCO_3$, although shown, are not included in the computation of the trend lines. The average <C–O> distance and <O–C–O> angle increase linearly with *V*, whereas the aplanarity of the CO_3 group decreases.

ACKNOWLEDGEMENTS

We thank D.J.M. Bevan, S. Ness, one anonymous referee, the Associate Editor, R.L. Flemming, and Editor, R.F. Martin for useful comments. We also thank D.H. Lindsley and R. Marr for their help with the EMP analysis. The HRPXRD data were collected at the X-ray Operations and Research beamline 11–BM, Advanced Photon Source (APS), Argonne National Laboratory (ANL). We thank J.S. Fieramosca for his help with the neutron-diffraction measurements, which were performed using the Special Environment Powder Diffractometer (SEPD), Intense Pulsed Neutron Source (IPNS), ANL. Use of the APS and IPNS was supported by the U.S. Department of Energy, Office of Science, Office of Basic Energy Sciences, under Contract No. DE–AC02–06CH11357. SMA acknowledges support from a University of Calgary grant, a Discovery grant RT735238 from the Natural Sciences and Engineering Research Council of Canada, and an Alberta Ingenuity New Faculty award.

REFERENCES

ANTAO, S.M. & HASSAN, I. (2007): $BaCO_3$: high-temperature crystal structures and the *Pmcn* → *R*3*m* phase transition at 811°C. *Phys. Chem. Minerals* **34**, 573-580.

ANTAO, S.M., HASSAN, I., MULDER, W.H. & LEE, P.L. (2008a): The $R\bar{3}c \rightarrow R\bar{3}m$ transition in nitratine, $NaNO_3$ and implications for calcite, $CaCO_3$. *Phys. Chem. Minerals* **35**, 545-557.

ANTAO, S.M., HASSAN, I., MULDER, W.H., LEE, P.L. & TOBY, B.H. (2009): In situ study of the $R\bar{3}c \rightarrow R\bar{3}m$ orientational disorder in calcite. *Phys. Chem. Minerals* **36**, 159-169.

ANTAO, S.M., HASSAN, I., WANG JUN, LEE, P.L. & TOBY, B.H. (2008b): State-of-the-art high-resolution powder X-ray diffraction (HRPXRD) illustrated with Rietveld structure refinement of quartz, sodalite, tremolite, and meionite. *Can. Mineral.* **46**, 1501-1509.

ANTAO, S.M., MULDER, W.H., HASSAN, I., CRICHTON, W.A. & PARISE, J.B. (2004): Cation disorder in dolomite, $CaMg(CO_3)_2$, and its influence on the aragonite + magnesite → dolomite reaction boundary. *Am. Mineral.* **89**, 1142-1147.

BERG, G.W. (1986): Evidence for carbonate in the mantle. *Nature* **324**, 50-51.

BEVAN, D.J.M., ROSSMANITH, E., MYLREA, D.K., NESS, S.E., TAYLOR, M.R. & CUFF, C. (2002): On the structure of

aragonite – Lawrence Bragg revisited. *Acta Crystallogr.* **B58**, 448-456.

BRAGG, W.L. (1924): The structure of aragonite. *Proc. R. Soc. London* **A105**, 16-39.

BRUKER (2000): SAINT, software reference manual. Bruker AXS, Madison, Wisconsin.

CASPI, E.N., POKROY, B., LEE, P.L., QUINTANA, J.P. & ZOLOTOYABKO, E. (2005): On the structure of aragonite. *Acta Crystallogr.* **B61**, 129-132.

CHEVRIER, G., GIESTER, G., HEGER, G., JAROSCH, D., WILDNER, M. & ZEMANN, J. (1992): Neutron single-crystal refinement of cerussite, $PbCO_3$, and comparison with other aragonite-type carbonates. *Z. Kristallogr.* **199**, 67-74.

COLBY, M.Y. & LACOSTE, L.J.B. (1933): The crystal structure of cerussite. *Z. Kristallogr.* **84**, 299-309.

DAL NEGRO, A. & UNGARETTI, L. (1971): Refinement of the crystal structure of aragonite. *Am. Mineral.* **56**, 768-772.

DEER, W.A., HOWIE, R.A. & ZUSSMAN, J. (1992): *An Introduction to the Rock-Forming Minerals* (2nd ed.). John Wiley, New York, N.Y.

DE VILLIERS, J.P.R. (1971): Crystal structures of aragonite, strontianite, and witherite. *Am. Mineral.* **56**, 758-767.

DICKENS, B. & BOWEN, J.S. (1971): Refinement of the crystal structure of the aragonite phase of $CaCO_3$. *J. Res. Nat. Bureau Stand.* **A75**, 27-32.

FINCH, A.A. & ALLISON, N. (2007): Coordination of Sr and Mg in calcite and aragonite. *Mineral. Mag.* **71**, 539-552.

HOLL, C.M., SMYTH, J.R., LAUSTSEN, H.M.S., JACOBSEN, S.D. & DOWNS, R.T. (2000): Compression of witherite to 8 GPa and the crystal structure of $BaCO_3$II. *Phys. Chem. Minerals* **27**, 467-473.

JAROSCH, D. & HEGER, G. (1986): Neutron diffraction refinement of the crystal structure of aragonite. *Tschermaks Mineral. Petrogr. Mitt.* **35**, 127-131.

JAROSCH, D. & HEGER, G. (1988): Neutron diffraction investigation of strontianite, $SrCO_3$. *Bull. Minéral.* **111**, 139-142.

LARSON, A.C. & VON DREELE, R.B. (2000): General Structure Analysis System (GSAS). *Los Alamos Nat. Lab., Rep.* **LAUR 86-748**.

LEE, P.L., SHU, D., RAMANATHAN, M., PREISSNER, C., WANG, J., BENO, M.A., VON DREELE, R.B., RIBAUD, L., KURTZ, C., ANTAO, S.M., JIAO, X. & TOBY, B.H. (2008): A twelve-analyzer detector system for high-resolution powder diffraction. *J. Synchr. Rad.* **15**, 427-432.

LIN CHUNG-CHERNG & LIU LIN-GUN (1997): High pressure phase transformations in aragonite-type carbonates. *Phys. Chem. Minerals* **24**, 149-157.

LUCAS, A., MOUALLEM-BAHOUT, M., CAREL, C., GAUDÉ, J. & MATECKI, M. (1999): Thermal expansion of synthetic aragonite condensed review of elastic properties. *J. Solid State Chem.* **146**, 73-78.

ONO, S. (2007): New high-pressure phases in $BaCO_3$. *Phys. Chem. Minerals* **34**, 215-221.

PILATI, T., DEMARTIN, F. & GRAMACCIOLI, C.M. (1998): Lattice-dynamical estimation of atomic displacement parameters in carbonates: calcite and aragonite $CaCO_3$, dolomite $CaMg(CO_3)_2$, and magnesite $MgCO_3$. *Acta Crystallogr.* **B54**, 515-523.

POKROY, B., FIERAMOSCA, J.S., VON DREELE, R.B., FITCH, A.N., CASPI, E.N. & ZOLOTOYABKO, E. (2007): Atomic structure of biogenic aragonite. *Chem. Mater.* **19**, 3244-3251.

RIETVELD, H.M. (1969): A profile refinement method for nuclear and magnetic structures. *J. Appl. Crystallogr.* **2**, 65-71.

SANTILLÁN, J. & WILLIAMS, Q. (2004): A high pressure X-ray diffraction study of aragonite and the post-aragonite phase transition in $CaCO_3$. *Am. Mineral.* **89**, 1348-1352.

SHANNON, R.D. (1976): Revised effective ionic radii and systematic studies of interatomic distances in halides and chalcogenides. *Acta Crystallogr.* **A32**, 751-767.

SHELDRICK, G.M. (1997): SHELXL–97–1. *Program for Crystal Structure Determination*. Institut fur Anorg. Chemie, Göttingen, Germany.

SHELDRICK, G.M. (2001): SADABS. *Program for the Siemens Area Detector Absorption*. Bruker AXS, Madison, Wisconsin.

SPEER, J.A. (1983): Crystal chemistry and phase relations of orthorhombic carbonates. *In* Carbonates: Mineralogy and Chemistry (R.J. Reeder, ed.). *Rev. Mineral.* **11**, 145-190.

TOBY, B.H. (2001): EXPGUI, a graphical user interface for GSAS. *J. Appl. Crystallogr.* **34**, 210-213.

WANG, J., TOBY, B.H., LEE, P.L., RIBAUD, L., ANTAO, S.M., KURTZ, C., RAMANATHAN, M., VON DREELE, R.B. & BENO, M.A. (2008): A dedicated powder diffraction beamline at the advanced photon source: commissioning and early operational results. *Rev. Sci. Instrum.* **79**, 085105.

WYCKOFF, R.W.G. (1925): Orthorhombic space group criteria and their applications to aragonite. *Am. J. Sci.* **209**, 145-175.

ZACHARIASEN, W.H. (1928): Untersuchungen über die Kristallstruktur von Sesquioxyden und vergindungen ABO_3. *Vid. Akad. Skr. Oslo* **4**, 1-165.

Received February 13, 2009, revised manuscript accepted October 6, 2009.